

Fundamental Symmetries and Conservation Laws

W. C. Haxton

Inst. for Nuclear Theory and Dept. of Physics, University of Washington, Seattle, WA 98195 USA

Abstract

I discuss recent progress in low-energy tests of symmetries and conservation laws, including parity nonconservation in atoms and nuclei, electric dipole moment tests of time-reversal invariance, β -decay correlation studies, and decays violating separate (family) and total lepton number.

Key words: parity nonconservation, electric dipole moments, correlations in β decay, lepton number
PACS: 11.30.Er, 11.30.Fs, 11.30.Hv, 14.60.Pq, 23.40.-s

1. Parity Nonconservation (PNC)

The use of parity in atomic spectroscopy dates from the 1920s, when it was introduced as a wave function label, prompting Wigner to demonstrate that such labeling is a consequence of the mirror symmetry of the electromagnetic interaction. Today parity and its violation are tools for probing aspects of the standard model (SM) (e.g., to isolate the strangeness-conserving hadronic weak interaction) and new physics beyond the SM (e.g., the contributions of a new boson Z'_0 to the running of weak couplings).

The weak interaction between atomic electrons and the nucleus is dominated by the coherent $A(e) - V(N)$ contribution. As the SM tree-level coupling to protons, $c_V(p) = 1 - 4\sin^2\theta_W \sim 0.1$, is suppressed while $c_V(n) = -1$, the weak charge of the nucleus $Q_{weak} \sim Zc_V(p) + Nc_V(n)$ is approximately $-N$. Consequently

$$H_{A(e)-V(N)}^{\text{Atomic PNC}} \sim \frac{G_F}{2\sqrt{2}} Q_{weak} \rho_N(\vec{r}) \gamma_5, \quad (1)$$

where $\rho_N(\vec{r})$ is the neutron density. The effects of this short-range interaction grow $\sim Z^3$ and thus are most easily detected in heavy atoms.

Atomic PNC was first observed in 1978, while the best current limit comes from the 1997 JILA experiment, $Q_{weak}({}^{133}\text{Cs}) = -73.16 \pm 0.29(\text{exp}) \pm 0.20(\text{theor})$ [1,2]. The $\sim 0.3\%$ precision poses a challenge for theoreticians attempting to calculate the associated

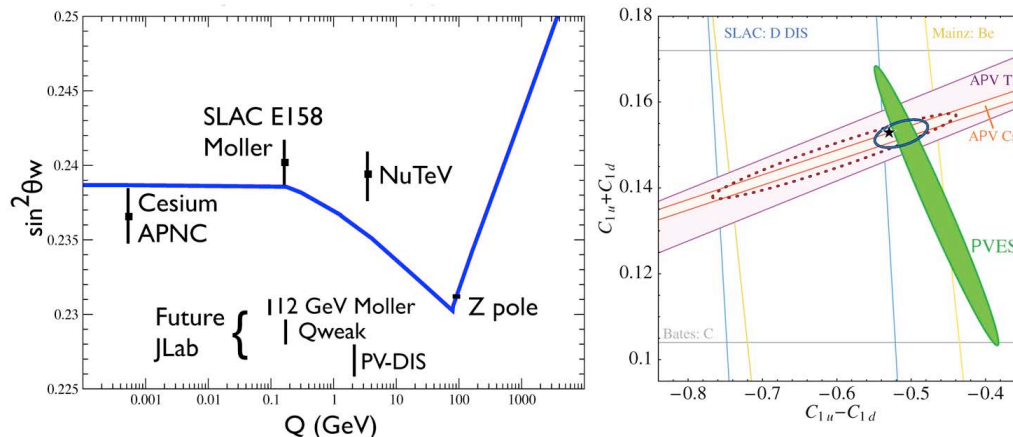


Fig. 1. In the left frame [4] experimental determinations of $\sin^2 \theta_W$ are compared to SM predictions, normalized to the Z pole. The right frame [3] shows the complementary constraints from atomic PNC ($Q_{weak} \sim N$) and PNC electron scattering (where protons have been the favorite target).

atomic mixing. Advances in the atomic structure calculations include improved evaluations of relativistic (Breit) and radiative corrections, vacuum polarization, the neutron distribution, strong-field self-energies, and weak vertex corrections. The corrections have been at the sub-1% level for Cs, and in total have brought SM calculations into agreement with experiment at $\lesssim 1\sigma$. Consequently beyond-the-SM contributions are constrained, yielding, e.g., a bound on the mass of an extra neutral boson, $M(Z'_0) \gtrsim 1.3$ TeV [2].

The atomic PNC constraint on $c_V(p)$ and $c_V(n)$, or equivalently on the underlying quark couplings, is essentially orthogonal to that from PNC electron scattering experiments, as shown in the right frame of Fig. 1 [3]. In the left frame experimental values for $\sin^2 \theta_W$ are superimposed on SM predictions for its running [4]. There is good agreement. Included on this graph are the error bars experimentalist expect to achieve in future intermediate-energy measurements at JLab.

The Cs experimenters also studied the hyperfine dependence of the signal, from which a small nuclear-spin-dependent contribution to PNC, $V(e) - A(N)$, was extracted,

$$H_{V(e)-A(N)}^{\text{Atomic PNC}} = \frac{G_F}{\sqrt{2}} \kappa \vec{\alpha} \cdot \vec{I} \rho(\vec{r}) \Rightarrow \kappa = \kappa_{Z_0} + \kappa_{\text{HF}} + \kappa_A = 0.112 \pm 0.016. \quad (2)$$

The measured κ , obtained from 7000 hours of data, constrains the sum of three terms, tree-level Z_0 exchange ($\kappa_{Z_0} \sim 0.014$, suppressed because the nuclear coupling is no longer coherent and the vector Z_0 coupling to the electron $\sim (4 \sin^2 \theta_W - 1)/2 \sim -0.05$ is small), spin-dependent effects arising from the combination of hyperfine and Q_{weak} interactions ($\kappa_{\text{HF}} \sim 0.0078$), and the nuclear anapole moment ($\kappa_A \sim 0.090 \pm 0.016$), which dominates the signal. The nuclear anapole moment is a PNC coupling of a photon to the nucleus (see Fig. 2), part of a set of weak radiative corrections. It arises from a PNC torroidal current winding within the nucleus, growing with atomic number as $A^{2/3}$ (proportional to the torroid's cross section). This growth leads to a the weak radiative correction that exceeds the tree-level axial Z_0 exchange in heavy nuclei.

Because the largest contribution to κ_A for a heavy nucleus comes from opposite-

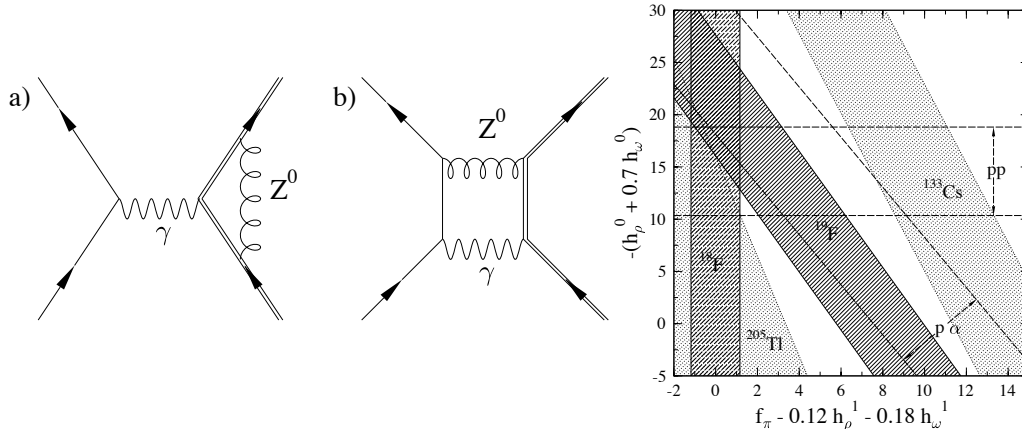


Fig. 2. The diagram on the left, a contribution to the anapole moment (a weak radiative correction arising from single-photon exchange), is part of a larger class of such corrections, including the box diagram at the center. The anapole constraints from atomic PNC studies of Cs and Tl are included in the diagram on the right, which summarizes the current status of hadronic PNC studies.

Table 1
S-P weak PNC amplitudes and the corresponding meson-exchanges [7]

Transition	$I \leftrightarrow I'$	ΔI	n-n	n-p	p-p	meson exchanges
$^3S_1 \leftrightarrow ^1P_1$	$0 \leftrightarrow 0$	0		x		ρ, ω
$^1S_0 \leftrightarrow ^3P_0$	$1 \leftrightarrow 1$	0	x	x	x	ρ, ω
		1	x		x	ρ, ω
		2	x	x	x	ρ
$^3S_1 \leftrightarrow ^3P_1$	$0 \leftrightarrow 1$	1		x		π^\pm, ρ, ω

parity admixtures in the ground-state nuclear wave function, κ_A provides a constraint on hadronic PNC. As discussed in the next section, the Cs anapole moment seems to be somewhat larger than one would expect based on other tests of hadronic PNC.

2. The Nucleon-Nucleon Parity-Nonconserving Interaction

The NN PNC interaction at low energies is characterized by the five S-P Danilov amplitudes of Table 1, which in turn are often parameterized in terms of a potential derived from ρ , ω , and π^\pm exchange [5]. This parameterization can be viewed as a phenomenological effective theory, with the heavy meson exchanges playing the role of short-range interactions $\vec{V}_{12}\delta(\vec{r}_{12})$ in each of the five S-P channels, and with the pion separately determining the long-range behavior of the potential (see Fig. 3). In fact, systematic effective field theory formulations exist for pionless theory and with explicit pions [6].

One of the goals of the field has been to isolate the neutral current contribution to hadronic PNC. While the weak interaction can be observed in flavor-changing hadronic decays, the neutral current contribution to such decays is suppressed by the GIM mechanism and thus unobservable. The NN and nuclear systems are thus the only practical laboratories for studying the hadronic weak interaction in all of its aspects [7].

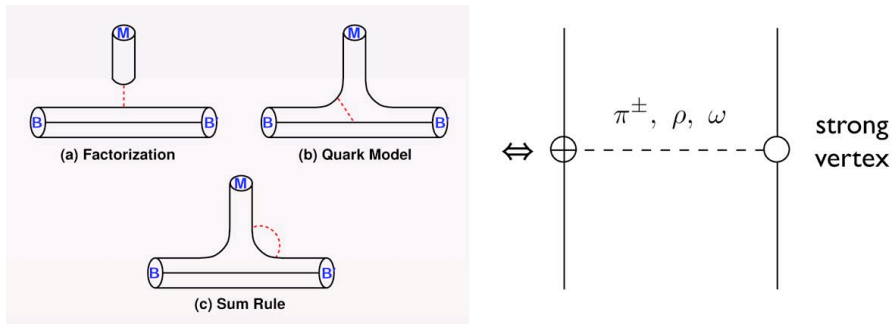


Fig. 3. A single-boson-exchange contribution to V_{PNC} contains one weak vertex (left) and one strong one (right). DDH [5] related the weak vertex to SM quark currents, using factorization, the quark model, and sum rules.

As the weak contribution to the NN interaction is much smaller than the strong and electromagnetic contributions, PNC is exploited to isolate weak effects. The most common observables are pseudoscalars arising from the interference of weak and strong amplitudes, e.g., the circular polarization of γ rays emitted from an unpolarized excited nuclear state, or the γ ray asymmetry if the nuclear state can be polarized. As the observable depends on a product of parity-conserving and PNC amplitudes, the weak interaction appears linearly. Alternatively, there are processes, such as the α decay of an unnatural-parity state to a 0^+ final state, where the observable depends on the square of a weak amplitude, and consequently is not a pseudoscalar.

The isospin of meson-nucleon couplings has an interesting relation to the underlying bare charged and neutral currents. The hadronic weak interaction is

$$L^{eff} = \frac{G}{\sqrt{2}} \left[J_W^\dagger J_W + J_Z^\dagger J_Z \right] + h.c. \quad J_W = \cos \theta_C J_W^{\Delta S=0} + \sin \theta_C J_W^{\Delta S=-1}, \quad (3)$$

where the charge-changing current is the sum of $\Delta I=1$ $\Delta S=0$ and $\Delta I=1/2$ $\Delta S=-1$ terms. Consequently the $\Delta S=0$ interaction has the form

$$L_{\Delta S=0}^{eff} = \frac{G}{\sqrt{2}} \left[\cos^2 \theta_C J_W^{0\dagger} J_W^0 + \sin^2 \theta_C J_W^{1\dagger} J_W^1 + J_Z^\dagger J_Z \right] \quad (4)$$

where the first term, a symmetric product of $\Delta I=1$ currents, has $\Delta I=0,2$, while the second term, a symmetric product of $\Delta I=1/2$ currents, is $\Delta I=1$ but Cabibbo suppressed. Consequently a $\Delta I=1$ PNC meson-nucleon vertex should be dominated by the neutral current term – a term not accessible in strangeness-changing processes. This is the π^\pm exchange channel. One could isolate this term by an isospin analysis of a complete set of PNC NN observables or, alternatively, by finding a case in which the isospins of the admixed nuclear states select only the $\Delta I=1$ contribution

Unfortunately, experimental progress in this field has been slow. Ideally one would like to avoid constraints from complex nuclei, as calculated nuclear mixing matrix elements are generally needed in the analysis. But there too few constraints available from NN and few-body experiments. The latest effort to improve this situation, the LANSCE measurement of the analyzing power $A_\gamma(\bar{n} + p \rightarrow d + \gamma)$, fell short of its goal and thus will need to be revisited when more intense neutron sources become available at the SNS. The best available data are [7]

$$\begin{aligned}
A_L(\vec{p} + p, 45 \text{ MeV}) &= (-1.57 \pm 0.23) \times 10^{-7} & P_\gamma(^{18}\text{F}) &= (12 \pm 38) \times 10^{-5} \\
A_L(\vec{p} + \alpha, 46 \text{ MeV}) &= (-3.34 \pm 0.93) \times 10^{-7} & A_\gamma(^{19}\text{F}) &= (-7.4 \pm 1.9) \times 10^{-5}
\end{aligned}$$

The mixing of nearly degenerate opposite parity doublets accounts for the large nuclear PNC signals. $P_\gamma(^{18}\text{F})$ is important because 1) the mixing is isovector and 2) the nuclear matrix element can be extracted from ancillary measurements (related axial-charge β decay) with very little uncertainty. The ^{19}F case is also partly constrained by similar data. Finally, there is the Cs anapole moment where, despite the apparent complexity of the nuclear structure physics, the existing theoretical analyses are in good accord.

The analyses of these data can be displayed as constraints on effective isoscalar and isovector weak couplings, as shown in the right panel of Fig. 2. If the Cs anapole moment is excluded, there is a region of overlap, corresponding to a small isovector coupling (compared to the “best value” of [5]) and an isoscalar coupling \gtrsim the DDH “best value.” The isovector coupling is constrained by the ^{18}F measurement and consistent with zero: this component is the test for neutral currents. But the conclusion of a suppressed isovector NN PNC interaction rests entire on this one measurement and associated analysis. When the ^{133}Cs anapole moment is added, no solution is found: the anapole moment appears to be larger than one would have expected, based on direct measurements of hadronic PNC. A small corner of the upper bound on the anapole moment of ^{205}Tl is also shown: while the error bar on the Tl measurement is quite large, the result favors a coupling opposite to that of ^{133}Cs , contradicting theory expectations.

Clearly the field needs a new generation of higher precision experiments, including neutron observables (e.g., in the $n + p$ system or $\vec{n} + ^4\text{He}$), to make progress.

3. Electric Dipole Moments and CP Violation

A permanent electric dipole moment d of an elementary particle or of a composite system (such as an atom) requires both time-reversal and parity violation: $H_{edm} = d \vec{E} \cdot \vec{s}$ reverses sign under $t \rightarrow -t$ and under $\vec{r} \rightarrow -\vec{r}$. The signature of an edm is precession of the particle’s spin around the direction of the applied field, with a frequency proportional to d and to the strength of the applied electric field. By the CPT theorem, a nonzero T-violating edm implies CP nonconservation (CPNC). Searches for edms

- test the SM’s two sources of CPNC, the CKM phase measured in neutral kaon decays and the unmeasured QCD θ parameter (edm searches require $|\theta| \lesssim 10^{-10}$); and
- probe CPNC beyond the SM (baryogenesis appears to require new sources).

The sensitivity of measurements is remarkable. The dipole moment limit for ^{199}Hg corresponds to a strain of about 10^{-19} , if interpreted in terms of a linear displacement. That is, were one to expand the atom to the dimensions of the earth, such an edm corresponds to a displacement of initially overlapping uniformly charged spheres (+ and -) by 10^{-4} angstroms. The Hg precession sensitivity, given typical electric fields of $\sim 10^5$ v/m, corresponds to shifts in energy level splittings of $\sim 10^{-26}$ eV.

The connection between experimental limits and fundamental Lagrangians is generally not simple. Particularly in the case of the edms of diamagnetic atoms – where the spin is carried by the nucleus – a theorist must relate the fundamental CPNC phases to effective low-energy couplings, determine the nuclear interactions these couplings induce, calculate the resulting CPNC mixing of nuclear states and thus the nuclear edm, and

Table 2

Edm limits, direct or derived, and expected SM level, based on the CKM phase [8,9].

Particle	edm limit	System	SM prediction (CKM phase)
e	1.9×10^{-27} e cm	atomic ^{205}Tl	10^{-38} e cm
p	6.5×10^{-23} e cm	molecular TlF	10^{-31} e cm
n	2.9×10^{-26} e cm	ultracold n	10^{-31} e cm
^{199}Hg	3.1×10^{-29} e cm	atom vapor cell	10^{-33} e cm

finally evaluate the atomic screening effects that determine the residual atomic edm, the quantity experimentalists measure.

The general electromagnetic current for a spin-1/2 fermion $\langle p' | j_\mu^{em} | p \rangle$ is

$$\bar{N}(p') \left(F_1(q^2) \gamma_\mu + F_2(q^2) \sigma_{\mu\nu} q^\nu + \frac{a(q^2)}{m^2} (\not{A} q_\mu - q^2 \gamma_\mu) \gamma_5 + d(q^2) \sigma_{\mu\nu} q^\nu \gamma_5 \right) N(p), \quad (5)$$

where F_1 and F_2 are the ordinary charge and magnetic couplings, a is the anapole coupling, and d the edm. In an atom or nucleus, this last term will generate odd static charge multipoles (C1 (the edm), C3, ...) and even static magnetic multipoles (M2, ...) that are CPNC and PNC (provide the spin allows M2 and C3 moments).

Edm experiments have been done on various neutral systems, including free neutrons, paramagnetic atoms or molecules (the unpaired electron provides sensitivity to the electron edm), and diamagnetic atoms (paired electrons but a nonzero nuclear spin, so that the valence nucleon's edm and CPNC nuclear state mixing can be probed). Table 2 lists some of the bounds. The field is quite active, with new or proposed efforts including ultracold neutrons (Ill, PSI, Munich, SNS), ^{199}Hg (Seattle), liquid ^{129}Xe (Princeton), trapped ^{225}Ra (Argonne, KVI) and ^{213}Ra (KVI), trapped ^{223}Rn , and the deuteron (BNL ring experiment). Future cold-neutron efforts, for example, may improve the current upper bound, 2.9×10^{-26} e cm, by a factor ~ 60 in the next decade [8].

A new result for ^{199}Hg , anticipated when this talk was delivered, has been announced. The experiment uses $\sim 10^{14}$ neutral atoms in a vapor cell designed to extend the spin relaxation time for Hg (which has atomic spin 0) to 100-200 s. The edm resides on the nucleus, which is shielded from an applied field by the polarization of the atomic cloud. Consequently a net interaction energy is generated only through nuclear finite-size effects, resulting in a reduced sensitivity to the nuclear edm,

$$d_{\text{atomic}} \sim 10Z^2 \left(\frac{R_N}{R_A} \right)^2 d_{\text{nucleus}}, \quad (6)$$

where R_N and R_A are the nuclear and atomic sizes. Such Schiff-shielding effects are less severe in heavy atoms, because of the stronger Coulomb field at the nucleus and larger R_N . The new result, $|d(^{199}\text{Hg})| \lesssim 3.1 \times 10^{-29}$ e cm [9], provides the most stringent bounds on a variety of possible sources of hadronic CPNC.

There are plans for a new generation of experiments employing trapped stable or radioactive isotopes. As traps allow more flexibility in the choice of nuclear and atomic spins, this technique may open up opportunities to exploit certain isotopes with enhanced polarizabilities (though higher spins may also increase sensitivity to field inhomogeneities). For example, the CPNC mixing of the 160 eV $5/2^-$ - $5/2^+$ ground-state parity doublet in ^{229}Pa is expected to enhance the nuclear edm by a factor of $\sim 10^3 - 10^4$

[10]. Theoretical studies of the collective enhancements of dipole moments of octupole-deformed nuclei, where parity doublets arise naturally [11], helped motivate Argonne and KVI proposals for ^{225}Ra .

4. Precise Measurements of Weak Decays

As approximately a dozen contributions to this conference discuss the use of precise decay measurements to probe the weak interaction, I wish there were more time available to discuss this field. There are several motivations for these difficult experiments:

- probing general properties of weak rates, such as universality, mixing angles (e.g., the extraction of V_{ud} from Fermi β decay or from the neutron), and coupling strengths (e.g., the pseudoscalar coupling F_P or the second-class tensor coupling F_T);
- constraining symmetry-breaking new interactions by their effects on muon or neutron decay, such as the exotic P-even, pseudo-T-odd neutron-decay D coefficient

$$\frac{d\omega}{dE_e d\Omega_e d\Omega_\nu} \propto p_e E_e (E_0 - E_e)^2 \left[1 + a \vec{\beta}_e \cdot \hat{p}_\nu + A \vec{\sigma}_n \cdot \vec{\beta}_e + B \vec{\sigma}_n \cdot \hat{p}_\nu + b \frac{m_e}{E_e} + D \vec{\sigma}_n \cdot (\vec{\beta}_e \times \hat{p}_\nu) \right]; \text{ and } \quad (7)$$

- verifying SM relations among decay parameters, e.g.,

$$a = \frac{g_V^2 - g_A^2}{g_V^2 - 3g_A^2} \quad A = -2 \frac{g_V^2 + g_A g_V}{g_V^2 - 2g_A^2} \quad B = 2 \frac{g_V^2 - g_A g_V}{g_V^2 - 3g_A^2}. \quad (8)$$

Nuclei can be useful in such tests: selection rules can simplify constraints. For example, in a high-Q $0^+ \rightarrow 0^+$ β decay, the back-to-back emission of the e^+ and ν_e is forbidden for a $V - A$ interaction because of unbalanced angular momentum associated with the handedness of the leptons. The addition of scalar (S, S') interactions

$$H_\beta = \bar{\psi}_n \gamma_\mu \psi_p \bar{\psi}_\nu C_V \gamma_\mu (1 - \gamma_5) \psi_e + \bar{\psi}_n \psi_p \bar{\psi}_\nu (C_S + C_{S'} \gamma_5) \psi_e \quad (9)$$

produces leptons with identical chiralities, so that emission in the same direction is forbidden, and back-to-back leptons preferred. Thus the daughter nucleus recoil momentum distribution (the observable) can be a sensitive test for nonzero C_S and $C_{S'}$. Among the interesting cases are ^{32}Ar [12] (where improved momentum resolution was achieved by measuring final-state delayed protons) and $^{38}\text{K}^m$ [13] (where a magneto-optical trap allowed the low-energy recoiling nucleus to freely escape to a detector).

5. Flavor and Total Lepton Number

The discovery of neutrino oscillations (e.g., $\nu_e \rightarrow \nu_\mu$) demonstrates that flavor is not conserved among the leptons and motivates further tests of lepton flavor number and total lepton number nonconservation,

$$\sum_{in} l_e \neq \sum_{out} l_e \quad \text{or} \quad \sum_{in} l_e + l_\mu + l_\tau \neq \sum_{out} l_e + l_\mu + l_\tau. \quad (10)$$

Total lepton number plays a special role in descriptions of neutrino mass.

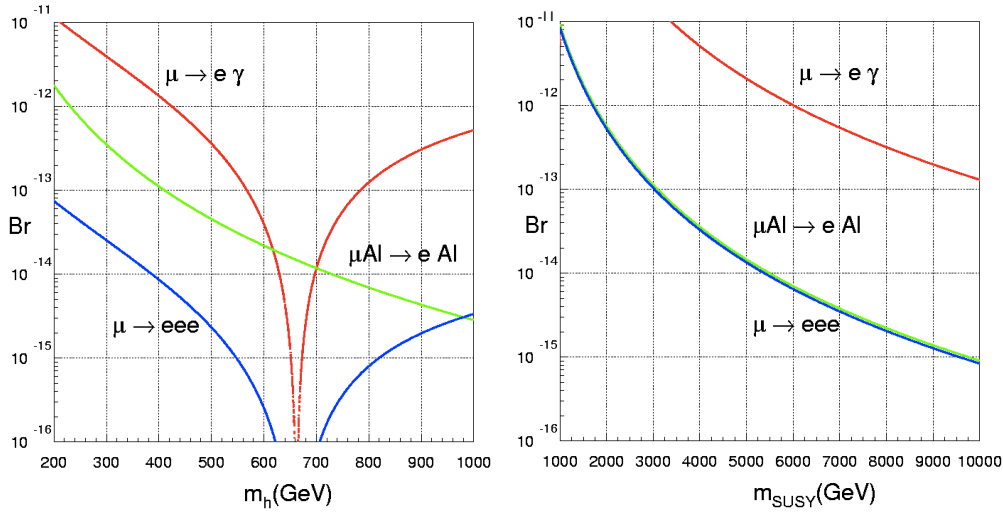


Fig. 4. Illustrations from [8,14] of the expected branching ratios for Higgs-mediated and gaugino-mediated LFV, vs. the respective Higgs boson and SUSY masses.

Table 3
Limits on LFV from experiments with muons [8]

Mode	Bound (90% c.l.)	Year	Experiment/Laboratory
$\mu^+ \rightarrow e^+ \gamma$	1.2×10^{-11}	2002	MEGA/LAMPF
$\mu^+ \rightarrow e^+ e^+ e^-$	1.0×10^{-12}	1988	SINDRUM I/PSI
$\mu^+ e^- \leftrightarrow \mu^- e^+$	8.3×10^{-11}	1999	PSI
$\mu^- \text{Ti} \leftrightarrow e^- \text{Ti}$	6.1×10^{-13}	1998	SINDRUM II/PSI
$\mu^- \text{Ti} \leftrightarrow e^+ \text{Ca}^*$	3.6×10^{-11}	1998	SINDRUM II/PSI
$\mu^- \text{Pb} \leftrightarrow e^- \text{Pb}$	4.6×10^{-11}	1996	SINDRUM II/PSI
$\mu^- \text{Au} \leftrightarrow e^- \text{Au}$	7.0×10^{-13}	2006	SINDRUM II/PSI

As the sources of lepton flavor violation (LFV) are varied, the relative sensitivities to new physics are highly model dependent. Classic low-energy tests include $\mu \rightarrow e + \gamma$, $\mu + (N, Z) \rightarrow e + (N, Z)$, and $\mu \rightarrow e + e + e$, as well as corresponding τ decays. Fig. 4 shows representative sensitivities for two LFV mechanisms.

Table 3 lists some of the LFV branching ratio bounds that have been obtained in the past two decades. The generally favored $\mu^+ \rightarrow e^+ \gamma$ mode can be mimicked by final-state accidentals, limiting the advantages of high-intensity muon beams. In contrast, as beam intensity is often a limiting factor in searches for $\mu^- \rightarrow e^-$ conversion in nuclei, improved beams can lead to large increases in sensitivity. The conversion process requires good energy resolution, $\lesssim 1$ MeV, to exclude the background from ordinary μ decay.

Both J-PARC and FermiLab have plans for next generation $\mu \rightarrow e$ conversion experiments that will substantially improve limits on LFV. These experiments will use pulsed proton beams to remove pion backgrounds by timing, large-acceptance capture solenoids to increase the μ flux, and bent solenoids to transport the muons, removing neutrals and separating charge. The FermiLab experiment will use 8 GeV protons from a new

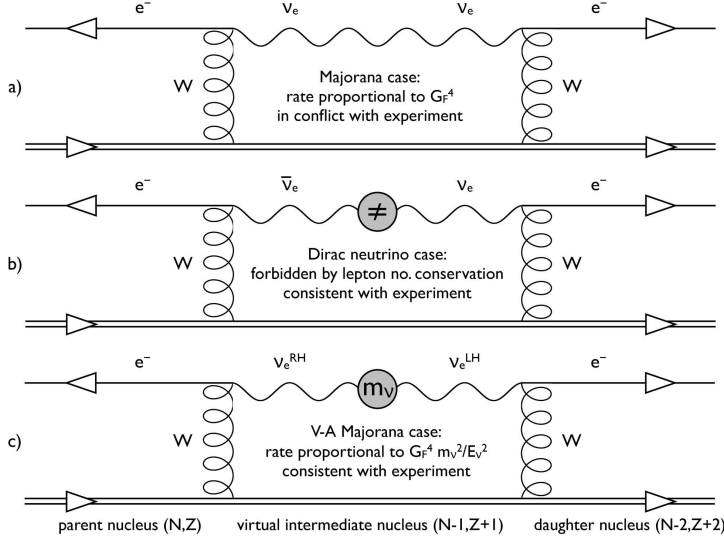


Fig. 5. Neutrinoless $\beta\beta$ decay scenarios: a) the pre-1957 Majorana case, which appeared to conflict with experiment; b) the Dirac case, where the process is forbidden by lepton number conservation; and c) the Majorana case, where the handedness mismatch is not total, due to the neutrino mass.

driver and has a branching ratio goal of 4×10^{-17} , while the J-PARC experiment will use a 40 GeV proton beam and has a goal of 5×10^{-19} [8]. This program will push LFV sensitivities for scalar exchanges from the current level of ~ 1 TeV to ~ 10 TeV.

Tests of total lepton number are important to the description of massive neutrinos. Neutrinos are unique among SM fermions in lacking an obvious charge or other additively conserved quantum number that would reverse sign under particle-antiparticle conjugation. Consequently, particle and antiparticle could be identical, $\nu = \bar{\nu}$. That is, the neutrino might be a Majorana particle, rather than Dirac ($\nu \perp \bar{\nu}$). Prior to 1957 the absence of neutrinoless $\beta\beta$ decay appeared to rule out a Majorana neutrino, since the process illustrated in Fig. 5a) would lead to relatively rapid decay. This result seemed to require a “charge” – lepton number – to distinguishing ν and $\bar{\nu}$, and the assumption of conservation of that charge to account for the absence of $\beta\beta$ decay,

$$l_e(e^-) = l_e(\nu_e) = +1 \quad l_e(e^+) = l_e(\bar{\nu}_e) = -1 \quad \sum_{in} l_e = \sum_{out} l_e. \quad (11)$$

The process in Fig. 5b) would then be forbidden, as there are no leptons in the initial state, while the final state carries a net lepton number of two.

But this conclusion ignores neutrino helicity: a massless right-handed neutrino has the wrong handedness to be reabsorbed in the second β decay of Fig. 5a). That is, absence of neutrinoless $\beta\beta$ tells us nothing about the Dirac or Majorana nature of the neutrino if the process is independently forbidden by maximal PNC.

The discovery of neutrino mass, however, changes this argument. Handedness is no longer exact and thus does not forbid $\beta\beta$ decay. Instead, the rate is suppressed by a factor $(m_\nu/E_\nu)^2$, where E_ν is the typical energy of the exchanged neutrino, as illustrated in Fig. 5c). If one can overcome this suppression factor by doing a very sensitive experiment,

$\beta\beta$ decay would be observed, provided Majorana neutrinos exist. Furthermore, the rate might tell us something about the scale of neutrino mass – important because oscillation experiments only probe m^2 differences.

One might expect the neutrino to have both Dirac $\bar{\Psi}_R M_D \Psi_L$ and Majorana $\bar{\Psi}_R^c M_R \Psi_R$ components. The latter breaks the global gauge invariance $\Psi \rightarrow e^{i\alpha} \Psi$ associated with a conserved lepton number l_e , and thus can contribute to manifestly l_e -forbidden processes like neutrinoless $\beta\beta$ decay. As was discussed in Concha Gonzalez-Garcia’s talk, there is a prejudice for such masses because they also explain, via the seesaw mechanism, why neutrinos are light. In the seesaw mechanism the diagonalization of the mass matrix

$$\begin{pmatrix} 0 & M_D \\ M_D & M_R \end{pmatrix} \longrightarrow m_\nu^{\text{light}} \sim M_D \left(\frac{M_D}{M_R} \right) \quad (12)$$

provides the needed “small parameter” M_D/M_R that explains why neutrinos are so much lighter than other SM fermions (which can only have Dirac masses). Thus light neutrinos are a reflection of the greater freedom available in building neutrino masses. Current oscillation results suggest $M_R \sim 3 \times 10^{15}$ GeV, a value near the GUT scale.

The possibility of discovering total-lepton-number violation is high because

- Nature likely makes use of Majorana masses;
- atmospheric neutrino experiments suggest that the mass scale is not unreasonably small, $m_\nu \gtrsim 0.05$ eV; and
- extraordinary efforts are underway to mount massive new $\beta\beta$ decay experiments that will extend current sensitivities by an additional factor ~ 1000 .

6. Summary

Precise tests of symmetries and conservation laws, using low-energy techniques, remain one of our best windows on physics of and beyond the SM, complementing the experiments performed at the energy frontier. Their utility derives from

- the many opportunities to isolate interesting interactions in both elementary and composite systems, using angular momentum, parity, and kinematics;
- exquisite experimental sensitivities (atomic shifts of $\sim 10^{-26}$ eV, $\beta\beta$ decay lifetimes of 10^{26} years);
- level degeneracies and collective responses enhancing interesting interactions in atoms and nuclei;
- unique sensitivities, such as the GUT-scale reach of $\beta\beta$ decay;
- the improving intensities of muon and cold neutron beams; and
- the capacity of theory to connect what is learned at low-energies to both astrophysics (e.g., neutrino mass) and accelerator physics (e.g., supersymmetry at the LHC).

7. Acknowledgment

This work was supported in part by the Office of Nuclear Physics, US Department of Energy. I thank the organizers of PANIC08 for a most enjoyable meeting.

References

- [1] C. S. Wood et al., *Science* **275**, 1759 (1997); S. C. Bennett and C. E. Wieman, *Phys. Rev. Lett.* **82**, 2484 (1999)
- [2] S. G. Porsev, K. Beloy, and A. Derevianko, arXiv: 0902.03351
- [3] R. D. Young, R. D. Carlini, A. W. Thomas, and J. Roche, *Phys. Rev. Lett.* **99**, 122003 (2007)
- [4] J. Erler and M. J. Musolf, *Phys. Rev. D* **72**, 073003 (2005)
- [5] B. Desplanques, J. F. Donoghue, and B. R. Holstein, *Annals Phys.* **124**, 449 (1980)
- [6] D. R. Phillips, M. R. Schindler, and R. P. Springer, arXiv:0812:2073; S. L. Zhu et al., *Nucl. Phys. A* **748**, 435 (2005)
- [7] E. G. Adelberger and W. C. Haxton, *Ann. Rev. Nucl. Part. Sci* **35**, 501 (1985)
- [8] M. Raidal et al., arXiv:0801:1826
- [9] W. C. Griffith, M. D. Swallows, T. H. Loftus, M. V. Romalis, B. R. Heckel, and E. N. Fortson, arXiv:0901.2328
- [10] W. C. Haxton and E. M. Henley, *Phys. Rev. Lett.* **51**, 1937 (1983); O. P. Sushkov, V. V. Flambaum, and I. B. Khriplovich, *Zh. Exp. Teor. Fiz.* **87**, 1521 (1984)
- [11] N. Auerbach, V. V. Flambaum, and V. Spevak, *Phys. Rev. Lett.* **76**, 4316 (1996); J. Dobaczewski and J. Engel, *Phys. Rev. Lett.* **94**, 232502 (2005)
- [12] E. G. Adelberger et al., *Phys. Rev. Lett.* **83**, 1299 (1999)
- [13] A. Gorelov et al., *Phys. Rev. Lett.* **94**, 142501 (2005)
- [14] P. Paradisi, *JHEP* **0608**, 047 (2006)